

RSC Advances



This is an *Accepted Manuscript*, which has been through the Royal Society of Chemistry peer review process and has been accepted for publication.

Accepted Manuscripts are published online shortly after acceptance, before technical editing, formatting and proof reading. Using this free service, authors can make their results available to the community, in citable form, before we publish the edited article. This *Accepted Manuscript* will be replaced by the edited, formatted and paginated article as soon as this is available.

You can find more information about *Accepted Manuscripts* in the [Information for Authors](#).

Please note that technical editing may introduce minor changes to the text and/or graphics, which may alter content. The journal's standard [Terms & Conditions](#) and the [Ethical guidelines](#) still apply. In no event shall the Royal Society of Chemistry be held responsible for any errors or omissions in this *Accepted Manuscript* or any consequences arising from the use of any information it contains.



Green synthesis of folic acid-conjugated gold nanoparticles with pectin as reducing/stabilizing agent for cancer theranostics†

Raja Modhugoor Devendiran^a, Senthil kumar Chinnaiyan^b, Narra Kishore Yadav^b, Ganesh Kumar Moorthy^c, Giriprasath Ramanathan^a, Sivakumar Singaravelu^a, Uma Tirichurapalli Sivagnanam^{a*}, Paramasivan Thirumalai Perumal^{d*}

Received 00th January 20xx,

Accepted 00th January 20xx

DOI: 10.1039/x0xx00000x

www.rsc.org/

In the present study pectin, a natural polysaccharide was employed for the one pot aqueous synthesis of gold nanoparticles (GNPs). Pectin acted concurrently as both a reducing and stabilizing agent. The formation of pectin reduced GNPs (Pec-GNPs) was confirmed by using a UV-visible spectrophotometer, with a characteristic surface plasmon resonance (SPR) band at 527 nm. EDS analysis proved the presence of gold in the sample. Spherical morphology and crystalline nature of the Pec-GNPs was demonstrated by TEM analysis. The FTIR spectrum revealed the capping of pectin on the surface of synthesised GNPs. Furthermore, the Pec-GNPs are found to be stable at different pH and electrolytic conditions. *In vivo* safety of the Pec-GNPs was established through zebra fish toxicity studies. Cationic drug doxorubicin was successfully loaded on the synthesized anionic Pec-GNPs by ionic complexation interaction. *In-vitro* release studies confirmed the pH dependent sustained release of the doxorubicin. Doxorubicin loaded Pec-GNPs exhibited enhanced *in vitro* cytotoxicity on the breast cancer cells over that of free doxorubicin, demonstrating that Pec-GNPs are efficient vehicles for the delivery of doxorubicin. Further Chitosan coupled with Folic acid (FA) was decorated with Pec-GNPs-DOX as a nanocarrier to improve the targeting and enhance the drug delivery to target cancer tissues by folic acid receptor-mediated endocytosis. It was concluded that the FA@Pec-GNPs-DOX were biocompatible and suitable for anti-cancer drug delivery, and were potentially promising as a new therapeutic system for cancer treatment.

1. Introduction

Cancer of the colon and rectum is one of the third most leading cancer causes 40 % of death in the world. Colon cancer cells when spread outside the colon or rectum to lymph nodes, they will reach to other lymph nodes, liver and many organs.¹ However the treatment of colon cancer includes surgery, radiofrequency ablation, cryosurgery, chemotherapy, radiation therapy. Thus, effective treatment demands increased dose size, which may lead to extreme

consequences. To improve this situation, pharmaceutical technologists have been working on metallic nanoparticles to deliver the drug more efficiently to the colon, where it can target the tumor tissues.²

Among the variety of metal nanoparticles, gold based nanomaterials are most extensively studied due to their unique optical, electronic characteristics and excellent biocompatibility.³ GNPs have wide variety of biomedical applications including drug delivery, medical diagnosis, photothermal therapy and biosensors.⁴⁻⁷ GNPs synthesized by conventional chemical and physical methods are mostly not suitable for biological applications as traces of unreacted reagents, or unwanted by-products are present in the colloidal gold solution prepared by these methods.⁸

Thus, recently much emphasis has been given to green synthesis methods in which non-toxic solvents and environmentally benign reducing and stabilizing agents was employed for the synthesis of GNPs.^{9, 10} Various plants,¹¹ polymers such as gellan gum,¹² chitosan,¹³ starch,¹⁴ hyaluronic acid¹⁵ and gum Arabic,¹⁶ guar gum¹⁷

a. Bioproducts Lab, CSIR-Central Leather Research Institute, Chennai-600020, Tamilnadu, India. E-mail: suma67@gmail.com; Tel: + 91 44 24420709; Fax: +91 44 24911589

b. Department of Pharmaceutical Technology, Anna University, BIT campus, Tiruchirappalli-620024, India.

c. Bio-Chemistry Lab, CSIR- Central Leather Research Institute, Adyar, Chennai-600020, India..

d. Organic Chemistry Division, CSIR-Central Leather Research Institute, Adyar, Chennai-600020, Tamilnadu, India. E-mail: piperumal@gmail.com; Fax: +91 44 24911539; Tel: + 91 44 24437223

†Electronic Supplementary Information (ESI) available: Figure

were used as reducing or stabilizing agents in the green synthesis of GNPs. Hydroxyl groups, hemiacetal reducing ends and other functionalities present in the natural polysaccharides play vital roles in both reduction and the stabilization of inorganic nanoparticles.¹⁸ Moreover, GNPs stabilized using different natural polymers are considered to be safe and biocompatible for various pharmaceutical and biological applications.¹⁹ There is a continuous search for suitable functionalizing agents for GNPs which play a dual role as effective reducing agent and promising stabilising agent, within an unprecedented reaction step.

Pectin (Pec) a structural plant polysaccharide contains 1, 4-linked α -D-galacturonic acid residues and finds an intensive application in the field of biomedicine due to biodegradable, biocompatible, and non-toxic characteristics.²⁰⁻²² By considering the importance for green synthesis and realizing the potential use of pectin in drug delivery, we have examined the synthesis of GNPs using pectin as both reducing and stabilising agent.

The use of pectin as reducing and capping agent to prepare GNPs in aqueous solutions is attractive as the procedure does not need the use of toxic chemicals and will yield GNPs that are biologically compatible and also suitable for drug delivery applications. Another major advantage of using pectin was that it will give the net anionic charge on the GNPs which could be exploited for easy loading of cationic drugs on Pectin reduced GNPs (Pec-GNPs) by simple electrostatic interaction. Reports are very few regarding the green synthesis of metal nanoparticles using pectin as both the reducing and stabilizing agent. For example, synthesis of iron oxide nanoparticles using pectin as the stabilising agent has been described.²³

The GNPs using microwave-assisted irradiation provided to have rapid and uniform heating with increased reaction kinetics and significantly improved experimental efficiency of the green synthetic methods.²⁴⁻²⁶

Doxorubicin (DOX) is a well-known antineoplastic drug effectively used for the treatment of various types of cancers.²⁷ To improve the safety and therapeutic efficacy of DOX, it can be delivered using specially designed nanocarriers that will selectively favor its accumulation in the target site and limit its distribution into healthy tissues.

The targeted drug delivery systems can lead to the reduction in the therapeutic dose of a drug and its toxic side effects. In addition, folate receptors (FR) were over-expressed in various human cancers, than most of the normal tissues.²⁸⁻²⁹ Folic acid (FA) is a commonly used as folate receptor ligand as it is a stable, low-cost, and poorly

immunogenic moiety having a very high affinity for the FR.³⁰ The decoration of nanocarriers with FA will improve the targeting ability of nanocarriers and enhance the drug delivery to target cancer tissues by folic acid receptor-mediated endocytosis with an intracellular delivery of anticancer agents than using a cell membrane marker which was not cell internalized.^{31,32}

In the present work DOX loaded on the pectin reduced GNPs and further decorated with chitosan coupled folic acid for the evaluation of anticancer activity against colon cancer cell line through specially designed nanocarriers.

2. Experimental methods

The chloroauric acid solution, Doxorubicin hydrochloride, Pectin, Chitosan (Molecular weight 150 kDa, deacetylation degree 85%), Folic acid, RPMI 1640 medium and 3-(4, 5-dimethylthiazol-2-yl)-2, 5-diphenyltetrazolium bromide (MTT), EDC, was purchased from Sigma-Aldrich, USA and used without further purification. NIH-3T3 fibroblasts and HT-29 colon cancer cells procured from National Centre for Cell Sciences (NCCS), Pune, India. E3 medium, a standard medium to work with Zebra fish embryos; (34.8 g NaCl, 1.6 g KCl, 5.8 g CaCl₂·2H₂O, 9.78 g MgCl₂·6H₂O, to prepare a 60 X stock solution. Dissolve the given amount of salts in 2 L of water. Adjust the pH to 7.2 with NaOH and autoclave it. To prepare 1X medium, dilute 16.5 mL of the 60 X stock solution to 1 L using sterile water). All experiments were performed in compliance with Committee for the Purpose of Control and Supervision of Experiments on Animals guidelines (CPCSEA), and performed after the approval from the Institutional Animal Care and Use Committee (IACUC).

Synthesis of pectin reduced gold nanoparticles

GNPs were synthesized by reducing the 1mM HAuCl₄ solution with 0.5 % w/v aqueous pectin solution (PS) by under microwave irradiation. 0.5 g of pectin was dissolved in 100 mL of distilled water and varying volumes of PS was added to 0.2 mL of 1 mM of HAuCl₄ solution and stirred well at room temperature. Followed by the microwave irradiation with the power of 700 W and heated for 8-10 min. The reaction mixture turned red wine colour indicating the formation of pectin reduced GNPs (Pec-GNPs). UV-Visible spectroscopic analysis was performed to confirm the formation of GNPs. Pec-GNPs was purified by removing the excess unreacted pectin by repeated washing with centrifuge operated at 18000 rpm for 20 min and the pellet was redispersed in deionised water. ICP-OES analysis was performed to know the concentration of gold in the sample.

Characterization techniques

Change in color was observed in the reaction mixture and the UV-visible spectra of the red solutions were recorded in a quartz cuvette with Analytica Jena UV-visible spectrophotometer, Germany. Morphology of the synthesized Pec-GNPs was analysed by FE-SEM analysis. Pec-GNPs solution was drop-cast on aluminium foil and air dried at 25 °C. The micrographs were taken in a Field emission Scanning electron microscope equipped with energy-dispersive X-ray spectroscopy. HRTEM images were recorded using FEI Tecnai G2 F20 S-Twin Transmission electron microscope. For the TEM analysis aqueous solution of synthesized GNPs was dropped onto a copper grid, dried under vacuum and micrographs were taken. The mean particle size was measured by Photon correlation spectroscopy (PCS) (Malvern Instruments 3000SH, UK). The sample was diluted with double distilled water to an appropriate scattering intensity. The surface charge of Pec-GNPs was determined by measurement of zeta potential. The lyophilized powder of Pec-GNPs was subjected to X-ray diffraction analysis (Seifert JSO-Debye flex 2002) at an operating voltage of 40 kV and a current of 30 mA with Cu K α_1 radiation (wavelength = 1.54056 Å). FTIR analysis was performed for freeze-dried Pec-GNPs, polymer pectin, DOX, Pec-GNPs-DOX and FA@Pec-GNPs-DOX. FTIR analysis of the samples was performed in an ABB 3000 Fourier transform infra-red spectrometer between 4000 and 400 cm⁻¹ using KBr pellet technique.

In vitro stability studies

0.5 mL of Pec-GNPs was incubated with 750 μ L of buffers (pH 1.2, pH 4.5, pH 6.8 and pH 7.4), normal saline. The 0.5 mL of Pec-GNPs incubated with deionized water was considered as control. The samples were kept at 37 °C for 48 h and were analyzed by UV-spectroscopy.

In vitro biocompatibility studies

In vitro cytotoxicity evaluation of Pec-GNPs was performed using fibroblasts cells. 1 X 10⁴ Cells at the log phase were seeded in wells of the cell culture plate containing DMEM medium and were incubated for 24 h at 37 °C and 5 % CO₂ environment. Various concentrations of Pec-GNPs (50, 75, 100, 125, 150 μ M) were added to the wells containing fibroblast cells and incubated in CO₂ incubator. Each test concentration was added to the test wells in triplicate manner. After 24 h incubation, MTT dye solution was added and kept for 4 h, and the formazan crystals so formed were dissolved using DMSO. The intensity of purple color was measured by micro plate reader at 570 nm wavelength. Untreated cells were considered as control.

In vivo Zebra fish toxicity studies

Zebra fish strains are maintained in clean water tanks in a 14 h light:10h dark cycle and allowed for natural mating. The resulted zebra fish embryos were collected and washed with E3 medium. 10 healthy embryos 6 h post-fertilization (hpf) was transferred per well in 96 well plates. Pec-GNPs diluted to a range of concentrations (200, 450, 600, 800 and 1000 nM) were added to wells containing zebra fish embryos and the plates were incubated. Percentage hatching rate and percentage survival rate was calculated to assess the toxicity effects of Pec-GNPs on zebra fish embryos. Moreover phenotype of the zebra fish embryos at 96 hpf was also studied using stereo microscope to find out the developmental abnormalities to understand the *in vivo* toxicity of Pec-GNPs.

Encapsulation efficiency

0.5 mL of stock solution (1mg/mL) of DOX was added to 2 mL of Pec-GNPs solution and kept under stirring for 8 h at 4 °C. Percentage drug loading was calculated by indirect method. The unbound DOX was removed by centrifugation process 18000 rpm for 15 min. Unbound DOX in the supernatant was determined by UV-Visible spectrophotometrically by measuring at 485 nm. The percentage drug loading was calculated by using the following formula.

% Encapsulation efficiency

$$= \frac{\text{Amt of DOX added initially} - \text{Amt of unloaded DOX in supernatant}}{\text{Amount of DOX added initially}} \times 100$$

Folic acid conjugation on DOX-Pec-GNPs

Folic acid (FA) (50 mg) was dissolved in 10 mL of 0.1 M of NaOH together with EDC (molar ratio 1:1) and kept under stirring for 3 h. To this add, 0.5% (w/v) chitosan solution (1% acetic acid) was added to this mixture and allowed to stir for 24 h, followed by dialysis against water to remove unreacted EDC, FA from Chitosan-FA conjugates. 10 mg of Chitosan-FA conjugate was added to Pec-GNPs-DOX and allowed to stir for 12 h followed by centrifugation to form folic acid functionalised DOX loaded GNPs (FA@Pec-GNPs-DOX).

The percentage of modified amino groups on the chitosan was determined by 2, 4, 6-Trinitrobenzene sulfonic acid (TNBSA) assay by detecting the remnant amino group on the chitosan molecules. The percentage of modified amino group on the chitosan was calculated by the following equation

$$\text{Modified percentage (\%)} = \frac{I_t - I_f}{I_t} \times 100$$

Where I_t and I_f were the absorbable intensity of the chitosan and chitosan conjugated with folic acid, respectively.

***In vitro* drug release characteristics**

Briefly FA@Pec-GNPs-DOX was taken in dialysis bag and immersed in 25 mL of phosphate buffer pH 7.4. The entire system was kept at 37 °C with continuous stirring at 50 rpm. sample was withdrawn at specific time intervals and DOX released was analyzed spectrophotometrically. Equal volume of fresh buffer was added every time after sample collection to maintain sink condition. The release studies were performed in triplicate.

Evaluation of anti-cancer activity using HT-29 cells

The cytotoxicity of DOX, Pec-GNPs-DOX, FA@Pec-GNPs-DOX on HT-29 cells was determined by conducting standard MTT assay. HT-29 cells (1×10^5 cells / well) were seeded in cell culture plates containing in RPMI-1640 medium and incubated at 37 °C, 5 % CO₂. Known concentrations (200, 400, 600, 800, 1000 and 1200 nM) of Pec-GNPs-DOX, FA@Pec-GNPs-DOX (equivalent to DOX) and free DOX was added to HT-29 cells and incubated. After 48 h the medium was removed and MTT solution was added and incubated for 4 h. After 4 h, DMSO was added to solubilise formazan crystals. The absorbance at 570 nm was measured using multiplate reader and cell viability was calculated. IC₅₀ concentration (concentration required for the inhibition of 50 % cell population) was found out to understand the cytotoxic activity of FA@Pec-GNPs-DOX. Cells incubated at same conditions without the test samples were considered as control. All experiments were performed in triplicate.

$$\% \text{ cell viability} = \frac{\text{Absorbance of test well}}{\text{Absorbance of control well}} \times 100$$

Apoptotic assay

The HT-29 cells were plated in 96 well plates (1×10^4 cells/well) and incubated at 37 °C in a humidified atmosphere of 5 % CO₂ incubator. Free DOX, Pec-GNPs, FA@Pec-GNPs-DOX were added in the wells and tested for their apoptotic activity. After incubation 10 µL of the AB/EB dye mixture (100 µg/mL of AO and 100 µg/mL of EB in phosphate buffer saline) was added to each well. The basic principle of live dead assay involves the usage of two fluorescent dyes acridine orange and ethidium bromide which specifically binds with live and dead cells, giving green and red fluorescence respectively. The excitation and emission maxima for acridine orange and ethidium bromide are 500/530, and 510/595 respectively. The apoptotic, necrotic and live cells were examined under the fluorescence microscope (OlympusCK40/U-RFLT50, Olympus, Japan). The experiment was performed in triplicate and the apoptotic cells were calculated.

DNA fragmentation analysis

HT-29 cells (1×10^6 cells) of log phase were seeded in to 6 well plates. The cells were treated with IC₅₀ concentration of the FA@Pec-GNPs-DOX and incubated. At the end of incubation cells were harvested and collected together along with non attached cells for the analysis of genomic DNA. The cells were shaken and cleared by centrifugation at 13000 rpm for 10 min. Cells were again suspended in 0.5 mL of lysis buffer (50 mM Tris-HCl, 100 mM EDTA, 0.5 % sodium dodecyl sulfate (pH 8.0) containing 0.1 mg/mL RNase A. After 30 min incubation at 37 °C, cells were treated with 1 mg/mL proteinase K for 10 min at 37 °C. DNA was extracted with phenol/chloroform and isoamylalcohol. DNA was precipitated using ethanol. By using 20 µL of TE buffer (10 mM Tris pH 7.5, 1 mM EDTA) DNA pellets were dissolved. By electrophoresis on a 1.5 % agarose gel for 1h at 80 V NA the samples were separated. The gel was stained with ethidium bromide, visualized under UV light, and photographed.

Western blot analysis

1×10^5 HT-29 cells at log phase were seeded onto 6-well plates. Cells were then treated with IC₅₀ concentration of FA@Pec-GNPs-DOX and incubated for a period of about 48 h. After 48 h cells were collected by trypsinization (cell lysis buffer containing 0.05 mol/l Tris-HCl (pH 7.5), 0.15 M NaCl, 0.001 mol/L PMSF, 0.001 M EDTA (pH 8.0), 1 % Triton X-100, 0.1 % SDS, 2 µg/mL leupeptin) and washed 3 times with PBS, and then centrifuged at 12000 rpm for 5 min at 4°C. The extracted protein samples (10 µg total protein/lane) were added in 5 times the volume of sample buffer and subjected to denaturation at 100°C for 10 min, then electrophoresed on SDS-PAGE (8 % for Bcl-2, 15%, caspases-3, and -9, β -actin) at 200 V for 45 min, and finally transferred on to PVDF membrane. The PVDF membrane was treated with PBS containing 5% skimmed milk at room temperature for 1h and then incubated with the primary antibodies anti Bcl -2 (dilution 1:2000), mouse monoclonal primary antibodies against anti-human Caspase 3 (1:2000), anti-human Caspase (1:2000), anti-human Bax (1:2000), anti Bcl 2 (1:1000), at 37 °C for 1 h at 4 °C overnight. After being washed 3 times with PBS for 15 min, 10 min, and 10 min respectively, the corresponding secondary antibody (dilution 1:2000) was added to it and incubated at room temperature for 1 h. The membrane was then washed 3 times for 15 min, 10 min, and 10 min respectively. After reacting with horseradish peroxidase-conjugated goat anti-mouse antibody, the immune complexes were visualized by using the chemiluminescence ECL PLUS detection reagents following the manufacturer's procedure.

Flow cytometric analysis

Cell cycle analysis was performed by cellular DNA content of HT-29 cells in the flow cytometer. HT-29 cells were grown to exponential phase, seeded at a density of 1×10^6 cells / six well dish, and treated with the IC_{50} concentration of FA@Pec-GNPs-DOX for 24 h. After treatment, the cells were collected by trypsinization, and fixed in ice-cold 70 % ethanol at -20°C overnight. The cells were resuspended in PBS containing 1 % Triton X-100, 0.5 mg/ml of RNase and 4 mg/mL of PI at 37°C for 30 min in dark room. Samples were analyzed for DNA content of 10000 cells per analysis using FACS Calibur flow cytometer, immediately after incubation (Becton Dickinson, San Jose, CA). The cell cycle was determined and analyzed using cell quest software.

3. Results and discussion

UV-Visible spectroscopic analysis

The UV-Visible spectrum of the synthesized Pec-GNPs. On microwave irradiation, reduction of Au^{3+} was visually confirmed as the reaction mixture finally turned to red colour within 10 min. Pec-GNPs were formed rapidly on microwave irradiation using pectin as reducing and stabilizing agent. Usually the microwave assisted method of synthesizing metal nanoparticles was advantageous as it will generate uniform localized heat at the reaction sites of the mixture and cause homogeneous nucleation and thereby increasing the rate of reaction resulting in the quick reduction of metal salts.¹³³
³⁴ The absorption spectra of Pec-GNPs were observed in the range of 500-600 nm (characteristic surface plasmon resonance zone of GNPs).³⁵ λ_{max} was occurred at 527 nm, which corresponds to the GNPs SPR band. Over all the UV- visible spectral analysis confirmed the formation of gold nanoparticles.

The optimum volume of PS needed for the reduction of HAuCl_4 (1mM), with their corresponding SPR was measured by UV-Visible spectroscopic analysis after microwave irradiation for 10 min. The

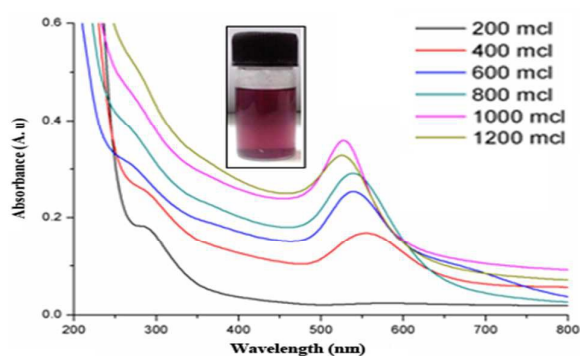


Fig. 1 UV-Visible spectra of Pec-GNPs

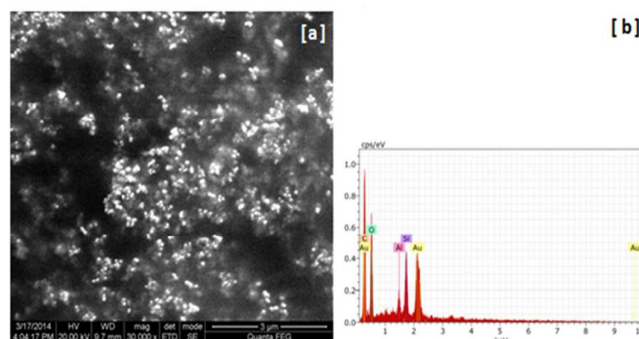


Fig. 2 (a) FE-SEM image of Pec-GNPs; (b) EDS of the Pec-GNPs

increase in intensity of the gold SPR band is quite distinct when PS volume was increased. The reason behind increase in intensity of SPR band with the increase in PS volume is because of the fact that the increase in number of pectin molecules facilitated the increased Au^{3+} reduction. Moreover from the UV-Vis spectra of Pec-GNPs (Fig.1) it is clear that at lower pectin volumes the SPR peak was broader indicating the presence of GNPs with broader size Distribution.³⁶ A blue shift was occurred in the SPR peak with the increasing volume of PS indicating the formation of smaller GNPs at higher volumes of PS. However, further increase in volume of PS to 1.2 mL lead to reduction in SPR peak intensity. It was decided that 1 mL of PS was the optimum volume which was sufficient to reduce the Au^{3+} used in the reaction. A possible reason was that there was a saturation point between the pectin and HAuCl_4 , which implied that the higher volumes of pectin solution inhibited the reduction process, and thus decreased the particle formation.

FE-SEM with EDS analysis

FE-SEM of Pec-GNPs under study is shown in Fig. 2(a) and it was found that Pec-GNPs have spherical morphology with narrow size distribution. Characteristic peak corresponding to Au was appeared in the EDS spectrum (Fig. 2(b)) and it confirmed the presence of gold in the sample. Other peaks corresponding to carbon and oxygen might have appeared due to the pectin polymer which was present on the surface of the GNPs as capping agent.

TEM analysis

TEM images Fig. 3(a-c) synthesised by microwave irradiation revealed that the most of the Pec-GNPs have nearly spherical shape and the average size was found to be 34 ± 8 nm. The selected area of electron diffraction pattern (SAED) of the Pec-GNPs showing the bright circular rings which corresponds to crystal lattice planes (111), (200), (220) and (311) of gold nano crystals (Fig. 3(d)) indicating that the synthesized GNPs are highly crystalline in nature.

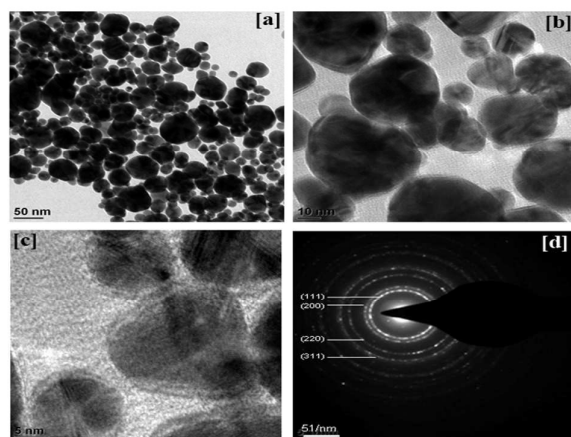


Fig. 3 (a-c) TEM image of Pec-GNPs, (d) SAED pattern of Pec-GNPs

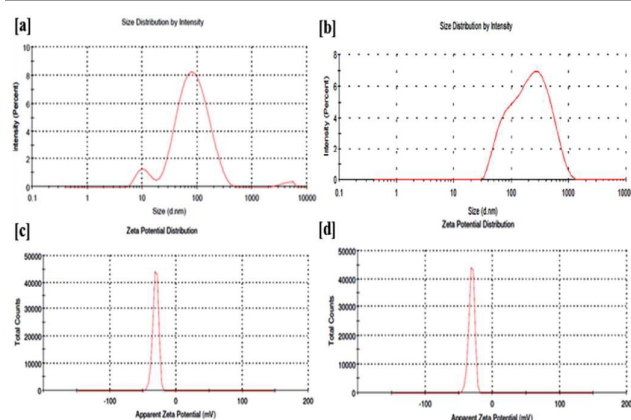


Fig. 4 (a) Particle size analysis of (a) Pec-GNPs by PCS showing the nanoparticles size distribution; (b) FA@Pec-GNPs-DOX by PCS showing the nanoparticles size distribution (c) Zeta potential distribution of Pec-GNPs; (d) Zeta potential distribution of Doxorubicin loaded Pec-GNPs

Particle size and Zeta Potential measurement

Average particle size of the Pec-GNPs and FA@Pec-GNPs-DOX was measured by PCS and it was found to be 56.17 nm and 150.5 nm (Fig. 4(a) and 4(b)). The particle size obtained from PCS analysis for Pec-GNPs and FA@Pec-GNPs-DOX was found to be 56 ± 3 nm and 150 ± 4 nm respectively. The qualitative analysis of the size of the nanoparticle was done by PCS analysis and observed to have difference of 94 nm thickness. This corresponds to the coating of FA-chitosan and drug over the surface of the Pec-GNPs. The Pec-GNPs exhibited to possess slightly bigger size PCS than TEM analysis (34 ± 8 nm). Samples were analyzed in dry state during TEM analysis whereas in PCS analysis hydrodynamic diameter of the nanoparticles were measured in liquid medium and therefore increase in particle size probably due to the swelling of hydrophilic pectin capped on the GNPs surface. Similar results were observed

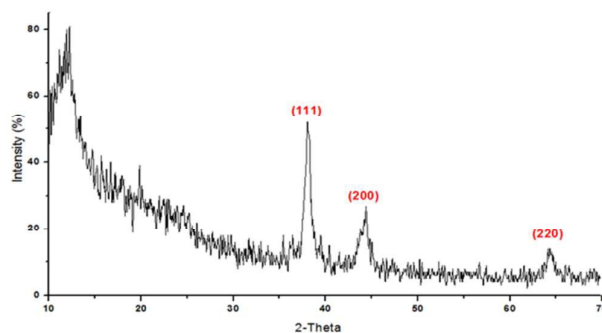


Fig. 5 XRD diffraction pattern of Pec-GNPs

during the synthesis of GNPs using heparin,³⁷ pullulan,^{38, 39} and chitosan.⁴⁰

Zeta potential of the synthesized Pec-GNPs was found to be -30.7 mV (Fig. 4(c)) and it gives the valuable information about the stability of colloidal aqueous dispersions. In general colloidal solutions having zeta potential above $+30$ mV or below -30 mV are considered stable.⁴¹ Negative zeta potential of synthesized Pec-GNPs can be ascribed to the capping by anionic pectin. Accordingly it was understood that Pec-GNPs were highly stable. Similarly zeta potential of DOX-Pec-GNPs was found to be -21.3 mV (Fig. 4(d)). The decrease in the zeta potential can be attributed to the DOX loading on the surface of Pec-GNPs. Earlier it was observed a slight reduction in zeta potential during the loading of positively charged DOX on anionic GNPs.⁴²

XRD Analysis

The X-ray diffraction pattern of Pec-GNPs formed by the reduction of HAuCl_4 with Pectin and irradiated with microwaves. The Bragg's reflection peaks at $2\theta = 37^\circ, 43^\circ, 65^\circ$ were predominant and can be indexed as (111), (200), (220) reflections of fcc structures of metallic gold. The results were comparable to the reported standard data (JCPDS file no. 04-0784) confirming that the GNPs were crystalline in nature (Fig. 5).

Determination of modified amino group and FTIR spectroscopy

The percentage of the modified amino group of the chitosan molecules exhibited about 58%.⁴³ The modified percentage of amino group were found to be medium and further they used for the preparation of FA@Pec-GNPs-DOX.

FTIR spectrum of folic acid (Fig. 6(a)) showed characteristic IR bands at $1699, 1607$ and 1483 cm^{-1} which are corresponding to the C=O, amino group in the pteridine ring and C=O or C=N bonds present in Folic acid. Similarly FTIR spectrum of chitosan (Fig. 6(b)) the characteristic peaks were observed at 3484 cm^{-1} (O-H stretch overlapped with N-H stretch), the absorption peaks in 1660 and 1604 cm^{-1} (amide I amide II group). Significant difference is

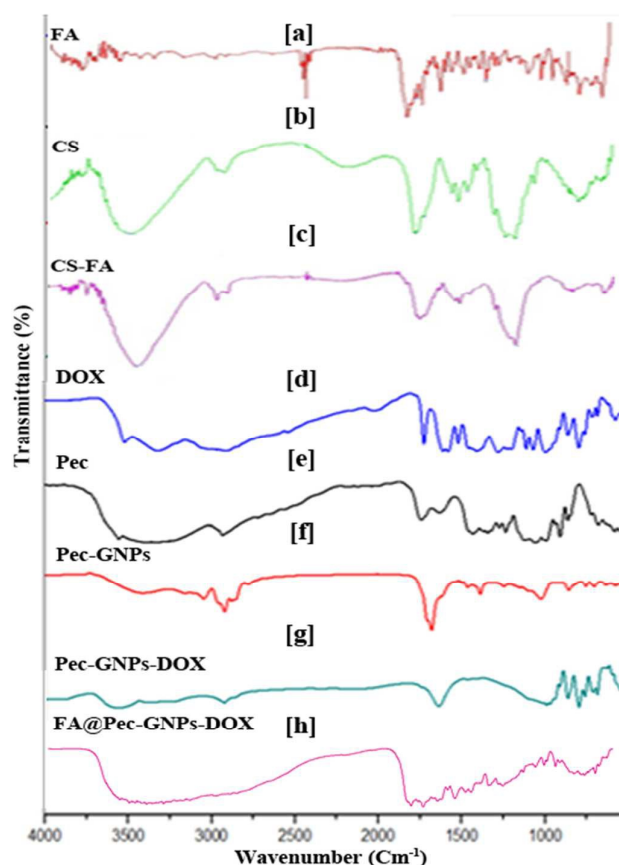


Fig. 6 FT-IR spectral analysis [a] Folic acid; [b] Chitosan; [c] Folic acid conjugated chitosan ; [d] Doxorubicin; [e] Pectin; [f] Pectin reduced GNPs; [g] Doxorubicin loaded pectin reduced GNPs; [h] Folic acid functionalized Doxorubicin loaded pectin reduced GNPs.

observed between the IR spectra of chitosan and chitosan conjugate folic acid. It can be seen (Fig. 6 (c)). The absorption peak at 1630 and 1026 cm^{-1} which belong to the vibration of C-N. The absorption peak of amide at 1660 cm^{-1} of chitosan shifts to 1630, which is overlapped with the absorption peak of the newly formed C-N bond which clearly indicates the coupling of folic acid to the chitosan. Fig. 6(d-h) represents the FT-IR spectra of Doxorubicin, Pectin, Pec-GNPs, Pec-GNPs-DOX and FA@Pec-GNPs-DOX respectively. Pectin shows characteristic peaks at 3000-3600 cm^{-1} indicated OH stretching, 2939 cm^{-1} corresponding to CH, 1748 cm^{-1} indicated carbonyl (C=O), and 1050 cm^{-1} corresponding, respectively -COC-stretching of the galactouronic acid. Similarly some typical characteristic peaks of pectin were found at 881 cm^{-1} (pyranose ring), 1274 cm^{-1} (C-O dilatation vibration), 1453 cm^{-1} (-CH₃ antisymmetric deformation or the -CH₂- symmetric deformation).^{42,44} Characteristic peaks of doxorubicin were found at 3524 cm^{-1} indicated the OH stretching, 2930 cm^{-1} indicated NH³⁺ stretching 1724 cm^{-1} , 1615 cm^{-1} , 1580 cm^{-1} indicated the C=O

stretching and the peaks found at 1000-1260 cm^{-1} (C-O stretching of alcohol) and 675-900 cm^{-1} (out of plane O-H bending).^{45, 46} Moreover presence of the characteristic peaks of pectin and doxorubicin with small shifts in Pec-GNPs and Pec-GNPs-DOX confirmed the presence of pectin and doxorubicin on the synthesized GNPs. Characteristic DOX- N-H group peak shifted to a higher value from 1615 to 1629 cm^{-1} confirms the interaction between doxorubicin and capping agent pectin. From the various literatures it was understood polysaccharides act as reducing and stabilizing agents in the synthesis of metallic nanoparticles through different mechanisms.⁴⁷ Hydroxyl groups and carboxyl groups which are abundantly present in polysaccharides play a vital role in reducing HAuCl₄ and stabilising the Au (0). Specifically the oxidation of hydroxyl groups to carbonyl groups cause the reduction of Au³⁺ to Au⁰ [54]. Moreover polysaccharides hydrolyze to some extent into monosaccharides, which in turn exist in cyclic and acyclic (aldehyde form) forms in aqueous medium. The aldehyde group may be responsible for the reduction of the metal ions.⁴⁸ Thus at this point of time it can be believed that pectin (a plant polysaccharide) acted as an excellent self-reducing and self-stabilizing agent through these one or more mechanisms and caused the reduction of HAuCl₄. But this observation toward different mechanisms has to be investigated further.

In vitro stability studies

The UV-Visible spectra of the Pec-GNPs incubated with different buffers and saline was shown in Fig. 7. There is a slight shift in the λ max of about 4 nm in the Pec-GNPs samples which were incubated with various biological buffer solutions (pH 4.5, 6.8 and 7.4) and normal saline. But in case of Pec-GNPs, incubated at pH 1.2 there is a shift in the λ max of about 8 nm with reduced peak intensity was observed.⁴⁹ Over all the results imply that Pec-GNPs possess

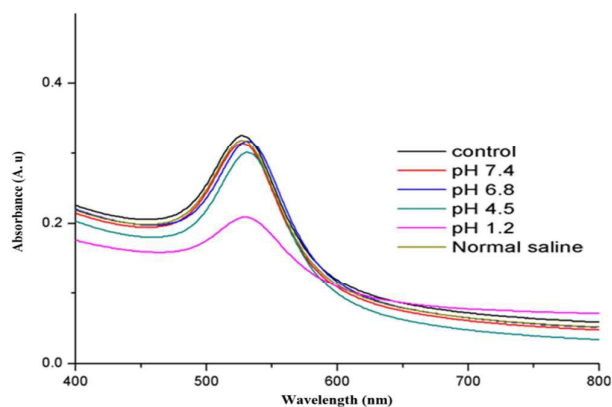


Fig. 7 UV-visible spectra of Pec-GNPs incubated with different buffers and saline

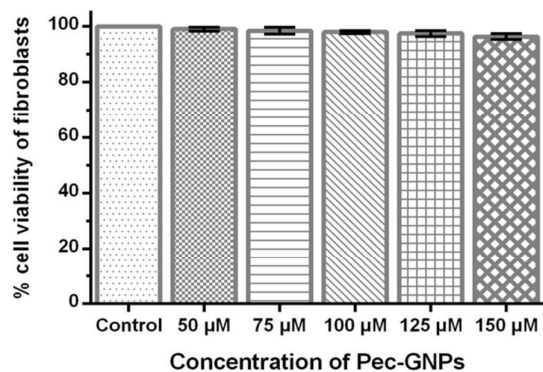


Figure 8 *In-vitro* biocompatibility studies showing the percentage cell viability of fibroblast cells incubated with Pec-GNPs. (Mean \pm S.D; n=3)

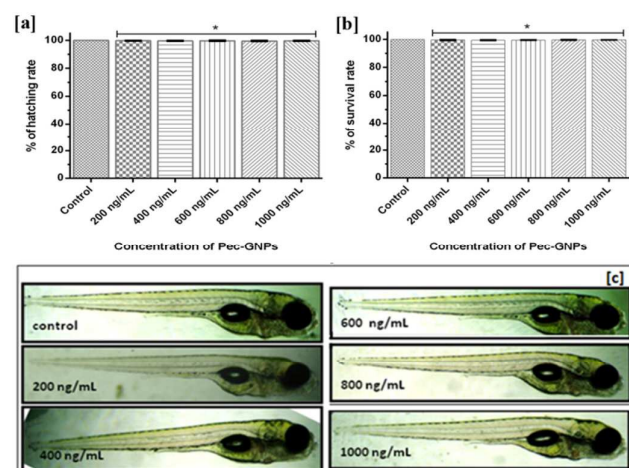


Fig. 9 (a) Graph representing the toxicity of Pec-GNPs in terms of hatching rate of larvae exposed to Pec-GNPs; (b) graph representing the toxicity of Pec-GNPs in terms of survival rate of larvae exposed to Pec-GNPs. (* $p < 0.05$; data presented are mean \pm SD, n =3); (c). Morphologic analysis of Pec-GNPs *in vivo* toxicity

remarkable *in vitro* stability in biological fluids at various pH and thus amenable to various therapeutic applications. *In vitro* biocompatibility studies

Since the synthesised Pec-GNPs were used as drug delivery carrier and so it becomes mandatory to establish their cytocompatibility. *In vitro* cytotoxicity of Pec-GNPs was analysed using fibroblast cell line and the results were shown in Fig. 8. After treatment with Pec-GNPs, cell proliferation was assessed by MTT assay. Upon treatment with Pec-GNPs (50 to 150 μ M), fibroblast cells showed more than 90 % viability which is almost comparable to the control (treated with PBS buffer (pH 7.4)) cells. This reveals that the pectin has provided a biocompatible coating onto GNPs and made them highly cytocompatible. Similar results were obtained for GNPs synthesised using biocompatible polymers such as bovine serum albumin⁵⁰, and glycol chitosan.⁵¹

In vivo Zebra Fish Toxicity studies

Zebra fish possess a high degree of homology to the human genome and it was considered as an inexpensive and useful *in vivo* model to evaluate the nanomaterials toxicity.^{52,53}

Zebra fish embryos were employed to understand the toxic effects of Pec-GNPs. The mortality rate and hatching rate was expressed in the Fig. 9(a) and Fig. 9(b). These studies clearly state, that there is no noticeable toxicity effect on hatching of Zebra fish embryos due to Pec-GNPs. Zebra fish embryos are transparent throughout every developmental stage and allowing direct observation of the development of all internal organs.⁵⁴

Pec-GNPs treated embryos were visualised using stereo microscope examination to study their morphology. Malformations such as pericardial oedema, yolk sac oedema, bent trunk and tail deformation was not seen in the Zebra fish embryos (Fig. 9 (c)). Hence, this investigation strongly suggests that the Pec-GNPs could be highly appropriate for biomedical and drug delivery applications.

Encapsulation efficiency of DOX and *in vitro* drug release studies

Doxorubicin was quickly encapsulated on the Pec-GNPs at room temperature. The negative charge of the Pec-GNPs has been exploited for encapsulating the positively charged doxorubicin on the GNPs surface through simple ionic interaction mechanism. Percent of encapsulation efficiency of DOX on to Pec-GNPs was determined based on DOX content in the supernatant after harvesting the DOX-encapsulated GNPs from the DOX solution. The amount of DOX bound on Pec-GNPs was found to be 85.56 ± 5.78 % (Fig. S1) Doxorubicin binding on to Pec-GNPs was further confirmed by the red shift happened in the SPR band towards higher wavelength from 527 nm to 535 nm.^{55,56} (Fig. 10)

In vitro release studies were performed under different pH conditions (pH 7.4 and pH 5.7) to measure DOX release from FA@Pec-GNPs-

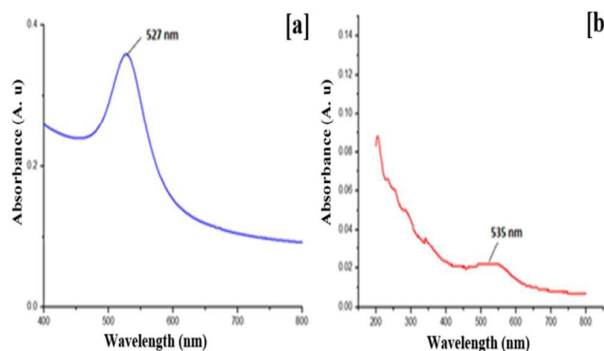


Fig. 10 UV-Visible spectra of [a] Pec-GNPs and [b] DOX loaded Pec-GNPs

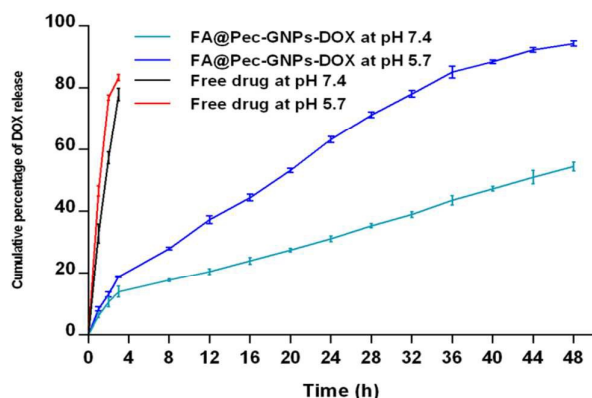


Fig. 11 *In vitro* release profiles of DOX from the DOX-Pec-GNPs and free DOX at different pH 5.7 and 7.4 at 37°C. (Mean \pm S.D; n=3)

DOX (Fig. 11). These pH conditions were selected particularly in this study to resemble the physiological characteristics such as blood (pH 7.4), acidic component of the tumour microenvironment and endosomes/ lysosomes.^{56, 57}

That DOX release from FA@Pec-GNPs-DOX was found to be slower than the release of free DOX. As shown in Fig. 11 more than 80 % of the free DOX was released in the first 4 h but the FA@Pec-GNPs-DOX exhibited a slow and controlled release of the drug. Moreover, DOX release was found to be dependent on the pH of the medium. At the end of 24 h, 65 % of the DOX was released at pH 5.7, whereas it was only 32% of DOX was released at pH 7.4. Thus, it is evident that FA@Pec-GNPs-DOX showed much faster DOX release at acidic pH than at physiological pH. Relatively low amount of DOX release from GNPs at pH 7.4 will ensure the decreased toxicity of DOX to the normal tissue. In general nanoparticulate delivery system exhibiting pH dependent release can be exploited for cancer drug delivery applications as the microenvironments of extracellular tissues of tumours and intracellular lysosomes and endosomes are acidic, and this acidity could facilitate active drug release from pH-dependent release carriers.^{58, 59}

Evaluation of Anti cancer activity

Standard MTT assay was employed to assess the anticancer activity of the free DOX and Pec-GNPs-DOX against HT-29 cells. Cell viability was calculated from the absorbance values measured at the end of 48 h incubation period. MTT assay results were shown in Fig. 12 demonstrate the free DOX and Pec-GNPs-DOX and FA@Pec-GNPs-DOX showed an increasing cytotoxicity against HT-29 cells in a dose-dependent manner.

The IC₅₀ value for Pec-GNPs-DOX, FA@Pec-GNPs-DOX was found to be 351 and 240 nM respectively while that for free DOX

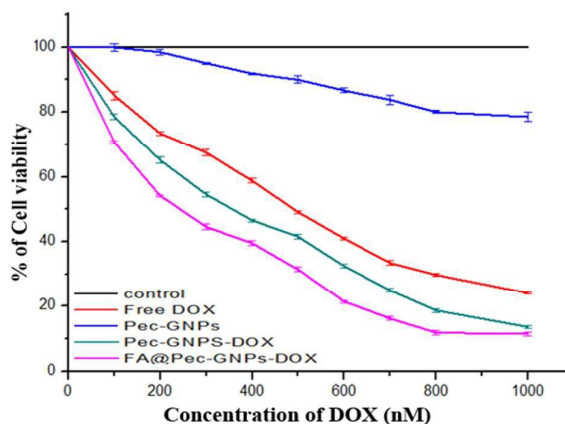


Fig. 12 Evaluation of Anti cancer activity in HT-29 colon cancer cells by MTT assay (Mean \pm S.D; n=3)

was found to be 483 nm in HT-29 cells. It can be confirmed that enhanced efficacy was observed with Pec-GNPs-DOX and FA@Pec-GNPs-DOX on the HT-29 colon cancer cells as the amount of DOX required to achieve 50% cell growth inhibition was much lower in the case of Pec-GNPs-DOX and FA@Pec-GNPs-DOX than free DOX. The superior cytotoxic activity of nanoparticulate doxorubicin could be due to the difference in uptake profile between free DOX, Pec-GNPs-DOX and FA@Pec-GNPs-DOX into the HT-29 colon cancer cells. Usually free drug molecules were transported into the cytoplasm of the cancer cell, by in a passive diffusion process, pumps, but if the drug was loaded in the suitable nanocarriers (Pec-GNPs) drug can enter into the cells by endocytosis mechanism which will result in higher cellular uptake of the entrapped drug molecules. This particular mechanism explains the enhanced cytotoxic activity of Pec-GNPs-DOX than the free DOX and similar effect was reported elsewhere.⁶⁰

Similarly, it can be understood that comparatively FA@Pec-GNPs-DOX showed better anticancer activity than Pec-GNPs-DOX. In the case of FA@Pec-GNPs-DOX, folic acid functionalized over the GNPs induced the particular binding of the GNPs to the folate receptors which were over expressed on the HT-29 cell surface. This binding might have facilitated the folate receptor-mediated endocytosis resulting in better cellular uptake of FA@Pec-GNPs-DOX by the HT-29 cells and thus, FA@Pec-GNPs-DOX exhibited superior cytotoxic activity than Pec-GNPs-DOX and free DOX. Therefore, it can be said that FA functionalization of the DOX-loaded Pec-GNPs played a significant role in enhancing the cytotoxic effect of DOX.^{61, 62}

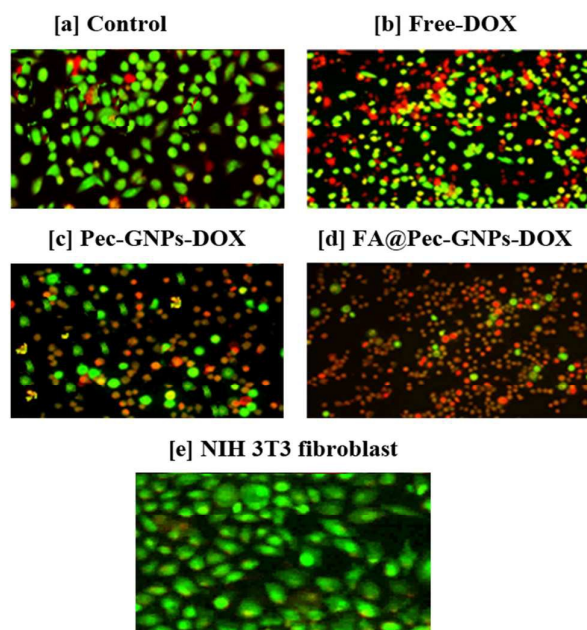


Fig. 13 Apoptosis assay by AO/EB staining method

Apoptosis Assay

Staining experiment using acridine orange (AO) and ethidium bromide (EB) was performed to investigate whether the cell death was caused by apoptosis process after the treatment with FA@Pec-GNPs-DOX. AO will stain both live and dead cells and it fluoresce green when bound to double stranded DNA in living cells and fluoresce red when bound to single-stranded DNA which dominates in dead cells. Also, EB stains only cells which have lost their membrane integrity and emits red fluorescence.^{63,64} Viable cells will have undamaged DNA and nucleus and exhibit round and green nuclei. Late apoptotic cells will have a fragmented DNA and exhibit red fluorescence. Microscopic images of the cells after staining were shown in Fig. 13. Control cells fluoresced uniformly green after the staining process indicating that they are in normal state. But HT-29 cells which were treated with FA@Pec-GNPs-DOX showed distinctive changes such as alteration in the shape of cells, cytoplasm shrinkage, contracted nucleus and condensed chromatin confirming the occurrence of apoptosis. Moreover, Fig. 13 clearly exhibited to have tremendously decreased the number of viable cells with a large number of later apoptotic cells (red coloured cells) were observed in the case of HT-29 cell population treated with FA@Pec-GNPs-DOX. Overall the results confirm that FA@Pec-GNPs-DOX caused a high degree of apoptosis than the free DOX. The cell-specific delivery of FA@Pec-GNPs-DOX was carried out through the apoptosis study in two different cell lines (HT-29 and NIH 3T3 fibroblasts cells). HT-29 cells are positive for folate receptors (FR

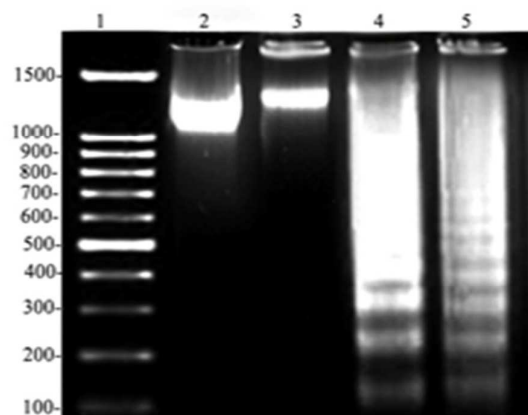


Fig. 14 Gel electrophoresis of DNA of HT-29 cells treated with. Lane 1: 1 kb ladder, Lane 2: control cells, Lane 3: Pec-GNPs, Lane 4: Free drug (DOX) Lane 5: FA@Pec-GNPs-DOX

Positive) and NIH 3T3 cells lack folate receptors (FR negative). It is usually known that folic acid coupled GNPs will have high affinity towards FA receptors which were expressed high on the cancer cells and thus deliver the drugs specifically to the cancer cells. Fig. 13 show that FA@Pec-GNPs-DOX did not produce any significant cell death confirming the cell-specific delivery characteristic of the folate-functionalized GNPs

DNA fragmentation assay

DNA was extracted from DOX, Pec-GNPs and FA@Pec-GNPs-DOX treated HT-29 colon cancer cells, and the presence of any necrosis was detected by agarose gel electrophoresis. It has been reported that during apoptosis, fragmented DNA gets fragmented and give rise to a series of bands called as "DNA ladders".⁶⁵ In Fig. 14 Lane 1 was loaded with the 1kb ladder. Lane 2, 3, 4 and 5 were loaded with an equal amount of DNA extracted from control HT-29 cells, Pec-GNPs, DOX and FA@Pec-GNPs-DOX respectively. DNA fragmentation was observed in the lane treated with DOX, and FA@Pec-GNPs-DOX indicating apoptosis in HT-29 cells. Moreover Fig. 14 Gel electrophoresis of DNA of HT-29 cells treated with Lane 1: 1 kb ladder, Lane 2: control cells, Lane 3: Pec-GNPs, Lane 4: Free drug (DOX) Lane 5: FA@Pec-GNPs-DOX was observed. However, DNA fragmentation has occurred to a greater extent in the sample of HT-29 cells treated with FA@Pec-GNPs-DOX than DOX revealing that FA@Pec-GNPs-DOX effectively caused cell death as compared to free DOX.

Cell cycle analysis

FACS analysis was performed to understand the effect of FA@Pec-GNPs-DOX on the progression of the cell cycle. The Flow cytometry results were showed in Fig. 15. It was observed that the

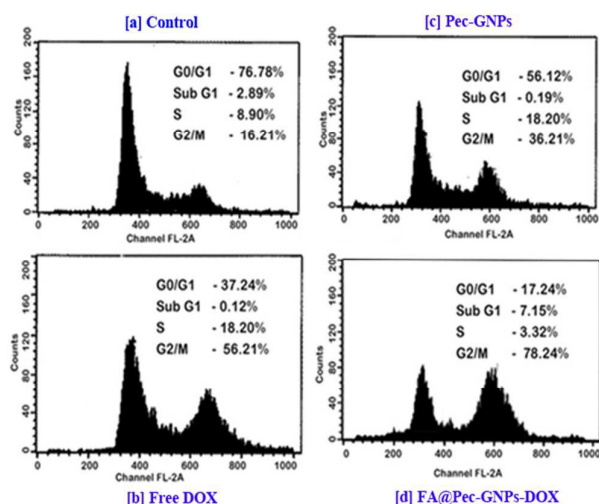


Fig. 15 Effects of FA@Pec-GNPs-DOX on HT-29 cell cycle analysis

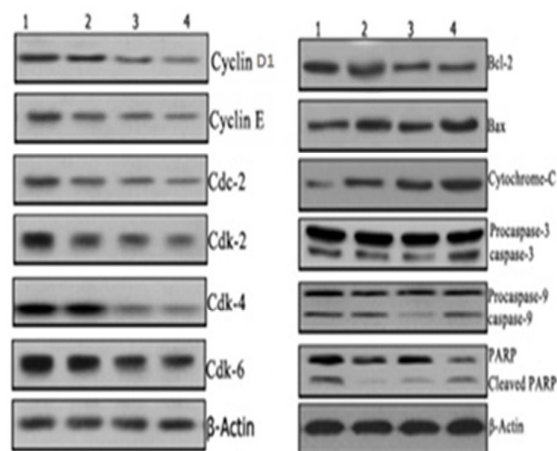


Fig. 16 Western blot illustrating the different protein expression in apoptosis after treatment with DOX and FA@Pec-GNPs-DOX. Lane 1: control, Lane 2: Pec-GNPs, Lane 3: Free drug DOX Lane 4: FA@Pec-GNPs-DOX

proportion of cells was increased in the G2/M phase after treatment with FA@Pec-GNPs-DOX indicating that FA@Pec-GNPs-DOX caused cell cycle arrest at the G2/M phase in HT-29 cells.⁶⁶

Western blot analysis

The key components of the cell cycle regulatory machinery are cyclins. Similarly CDK1-4, 6, 10, 11 have the direct role in the cell cycle progression.⁶⁷ Cell cycle expressions of regulatory proteins such as cyclinD1 and cyclin E and cyclin-dependent kinases such as CDK2, CDK4, CDK6 that regulate the different phases of the cell cycle were also evaluated.

Fig. 16 reveal that FA@Pec-GNPs-DOX treatment down-regulated the expression of cyclinD1 and Cyclin E. Similarly it was observed that there was a down-regulation of Cdk-4 and Cdk-2 in HT-29 cells after FA@Pec-GNPs-DOX treatment. These results indicate that

FA@Pec-GNPs-DOX caused death in HT-29 colon cancer cells by inducing apoptosis process. In this study, β -actin was used as a loading control, and it showed similar expression in all lanes. The expression of Bcl-2 protein, Bax protein was investigated to understand whether FA@Pec-GNPs-DOX caused the cell death through any receptor-mediated mechanism. In the present investigation, it was clear that FA@Pec-GNPs-DOX had induced down-regulation of Bcl-2 proteins and up-regulation of Bax proteins in HT-29 colon cancer cells.

Caspases, a family of cysteine acid proteases, can be regarded as the critical factors in apoptosis⁶⁸ and moreover cleaved form of PARP facilitates cellular disassembly and serves as a marker of apoptotic cells.⁶⁹ In the present study cleavage of caspase 9, caspase 3 and PARP proteins were observed in the case of Fa@Pec-GNPs-DOX treated cells, and these results confirmed the occurrence of apoptosis.

4. Conclusion

In the present study pectin, a natural polysaccharide was successfully employed for the one pot aqueous synthesis of gold nanoparticles (GNPs). Pectin acted concurrently as both a reducing and stabilizing agent. The Pec-GNPs exhibited a characteristic surface plasmon resonance (SPR) band at 527 nm with spherical morphology. The GNPs showed better *in vivo* toxicity studies using Zebra fish. Cationic drug doxorubicin loaded on the synthesized anionic Pec-GNPs exhibits excellent stability at different pH and electrolytic condition with the pH dependent sustained release of the doxorubicin. Folic acid was conjugated to the doxorubicin loaded Pec-GNPs to achieve active targeting of HT-29 colon cancer cells with excellent cytotoxicity. Flow cytometry analysis revealed that FA@Pec-GNPs-DOX caused the death of HT-29 cells by G2/M phase arrest. Overall the *in vitro* drug release, cytotoxicity, therapeutic efficacy results showed that FA@Pec-GNPs-DOX could be a promising alternative carrier for targeting colon cancer. It can be expected that under *in vivo* due to their nano-sized FA@Pec-GNPs-DOX will accumulate in the tumor tissue preferentially through the EPR (Enhanced Permeability and Retention) effect and folate targeting mechanism which will significantly enhance the efficacy of doxorubicin.

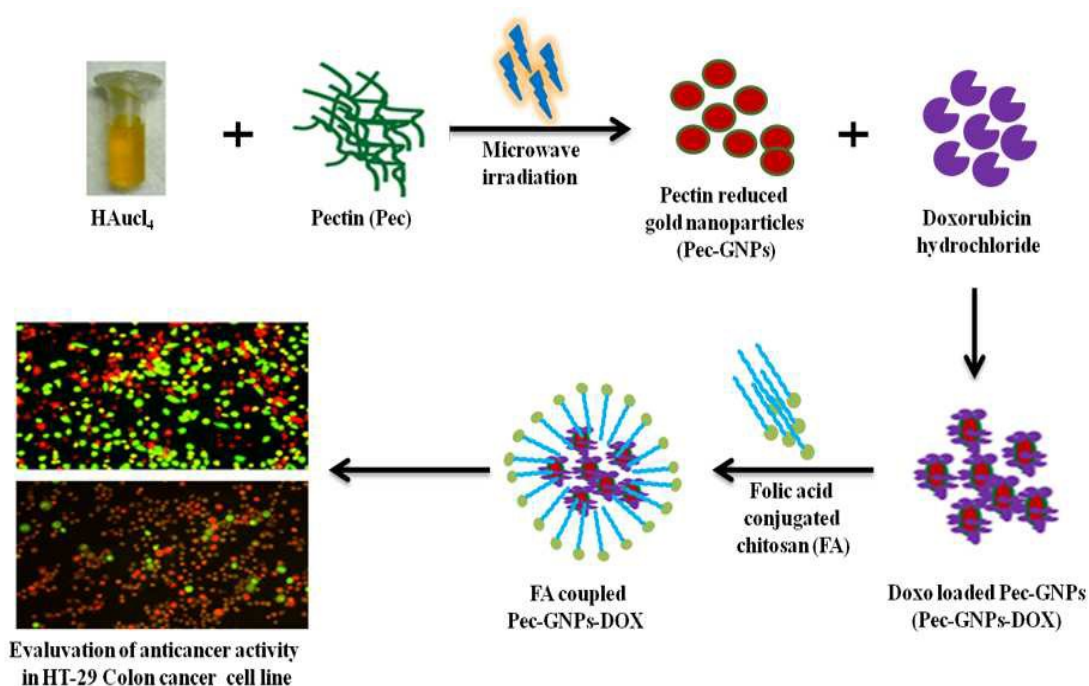
Acknowledgments

The author Raja M. D thanks Council of Scientific and Industrial Research (CSIR), New Delhi, India, for providing the funds to carry out this study.

Reference

- [1]. Chaurasia, M., Chourasia, M. K., Jain, N. K., Jain, A., Soni, V., Gupta, Y., & Jain, S. K., *Aaps Pharmscitech.*, 2006, 7, E143-E151.
- [2]. Anitha, A., Sreeranganathan, M., Chennazhi, K. P., Lakshmanan, V. K., & Jayakumar, R., *European Journal of Pharmaceutics and Biopharmaceutics*, 2014, **88**, 238-251.
- [3]. Guo, R., Zhang, L., Zhu, Z., & Jiang, X., *Langmuir*, 2008, **24**, 3459-3464.
- [4]. Aromal, SA., Vidhu, VK., & Philip, D., *Spectrochimica Acta Part A: Molecular and Biomolecular Spectroscopy*, 2012, **85**, 99-104.
- [5]. Devi, PS., Banerjee, S., Chowdhury, SR., & Kumar, GS., *RSC Advances*, 2012, **2**, 11578-11585.
- [6]. Richards, SJ., & Gibson, MI., *ACS Macro Letters*, 2014, **3**, 1004-1008.
- [7]. Noruzi, M., Zare, D., & Davoodi, D., *Spectrochimica Acta Part A: Molecular and Biomolecular Spectroscopy*, 2012, **94**, 84-88.
- [8]. Das, RK., Sharma, P., Nahar, P., & Bora, U., *Materials Letters*, 2011, **65**, 610-613.
- [9]. Maity, S., Sen, I. K., & Islam, S. S., *Physica E: Low-dimensional Systems and Nanostructures*, 2012, **45**, 130-134.
- [10]. Venkatpurwar, V., Shiras, A., & Pokharkar, V., *International journal of pharmaceutics*, 2011, **409**, 314-320.
- [11]. Irvani, S., *Green Chemistry*, 2011, **13**, 2638-2650.
- [12]. Dhar, S., Mali, V., Bodhankar, S., Shiras, A., Prasad, BLV., & Pokharkar, V., *Journal of Applied Toxicology*, 2011, **31**, 411-420.
- [13]. Wei, D., & Qian, W., *Colloids and Surfaces B: Biointerfaces*, 2008, **62**, 136-142.
- [14]. Pienpinijtham, P., Thammacharoen, C., & Ekgsit, S., *Macromolecular Research*, 2012, **20**, 1281-1288.
- [15]. Kemp, MM., Kumar, A., Mousa, S., Park, TJ., Ajayan, P., Kubotera, N., Mousa, SA., Linhardt, RJ., *Biomacromolecules*, 2009, **10**, 589-595.
- [16]. Devi, PR., Kumar, CS., Selvamani, P., Subramanian, N., & Ruckmani, K. (2015). *Materials Letters*, 2015, **139**, 241-244.
- [17]. Pandey, S., Goswami, GK., & Nanda, KK., *Carbohydrate polymers*, 2013, **94**, 229-234.
- [18]. Sathiyarayanan, G., Vignesh, V., Saibaba, G., Vinothkanna, A., Dineshkumar, K., Viswanathan, MB., & Selvin, J., *RSC Advances*, 2014, **4**, 22817-22827.
- [19]. Hien, NQ., Van Phu, D., & Duy, NN., *Carbohydrate polymers*, 2012, **89**, 537-541.
- [20]. Das, S., Chaudhury, A., & Ng, KY., *Journal of microencapsulation*, 2011, **28**, 268-279.
- [21]. Liu, L., Fishman, ML., Kost, J., & Hicks, KB., *Biomaterials*, 2003, **24**, 3333-3343.
- [22]. Meneguín, AB., Cury, BSF., & Evangelista, RC., *Carbohydrate polymers*, 2014, **99**, 140-149.
- [23]. Ngeneleme, FTJ., Eko, NJ., Mbom, YD., Tantoh, ND., & Rui, KW., *Open Journal of Composite Materials*, 2013, **3**, 30-37.
- [24]. Chen, J., Wang, J., Zhang, X., & Jin, Y., *Materials Chemistry and Physics*, 2008, **2**, 421-424.
- [25]. Hu, B., Wang, SB., Wang, K., Zhang, M., & Yu, SH., *The Journal of Physical Chemistry C*, 2008, **112**, 11169-11174.
- [26]. Kahrilas, GA., Wally, LM., Fredrick, SJ., Hiskey, M., Prieto, AL., & Owens, JE., *ACS Sustainable Chemistry & Engineering*, 2013, **2**, 367-376.
- [27]. Unsoy, G., Khodadust, R., Yalcin, S., Mutlu, P., & Gunduz, U., *European Journal of Pharmaceutical Sciences*, 2014, **62**, 243-250.
- [28]. Hidaka, M., Kanematsu, T., Ushio, K., & Sunamoto, J., *Journal of bioactive and compatible polymers*, 2006, **21**, 591-602.
- [29]. Elnakat, H., & Ratnam, M., *Advanced drug delivery reviews*, 2004, **56**, 1067-1084.
- [30]. Yang, SJ., Lin, FH., Tsai, HM., Lin, CF., Chin, HC., Wong, JM., & Shieh, MJ., *Biomaterials*, 2011, **32**(8): 2174-2182.
- [31]. VanHaandel, L., & Stobaugh, JF., *Analytical and bioanalytical chemistry*, 2010, **397**, 1841-1852.
- [32]. Stella, B., Arpicco, S., Peracchia, MT., Desmaële, D., Hoebeke, J., Renoir, M., & Couvreur, P., *Journal of pharmaceutical sciences*, 2000, **89**, 1452-1464.
- [33]. Bhuvanaree, SR., Harini, D., Rajaram, A., & Rajaram, R., *Spectrochimica Acta Part A: Molecular and Biomolecular Spectroscopy*, 2013, **106**, 190-196.
- [34]. Peng, H., Yang, A., & Xiong, J., *Carbohydrate polymers*, 2013, **91**, 348-355.
- [35]. Liu, J., Liu, R., Li, H., Kong, W., Huang, H., Liu, Y., & Kang, Z., *Dalton Trans.*, 2014, **43**, 12982-12988.
- [36]. Wu, CC., & Chen, DH., *Gold Bulletin*, 2010, **43**, 234-240.
- [37]. Sun, IC., Eun, DK., Na, JH., Lee, S., Kim, IJ., Youn, IC., Ko, CY., Kim, HS., Lim, D., Choi, K., Messersmith, PB., Park, TG., Kim SY., Kwon, IC., Kim, K & Ahn, CH., *Chemistry-A European Journal*, 2009, **15**, 13341-13347.

- [38]. Ganeshkumar, M., Ponrasu, T., Raja, MD., Subamekala, M. K., & Suguna, L., *Spectrochimica Acta Part A: Molecular and Biomolecular Spectroscopy*, 2014, **130**, 64-71.
- [39]. Komalam, A., Muraleegharan, LG., Subburaj, S., Suseela, S., Babu, A., & George, S., *International Nano Letters*, 2012, **2**, 26.
- [40]. Mirza, A. Z., & Shamshad, H., *European journal of medicinal chemistry*, 2011, **46**, 1857-1860.
- [41]. Vinod Venkatpurwar, Anjali Shiras, Varsha Pokharkar *International Journal of Pharmaceutics*. 2011, **409**, 314–320.
- [42]. Kumar, A., & Chauhan, GS., *Carbohydrate Polymers*, 2010, **82**, 454-459.
- [43]. Shu-Jyuan Yang, Feng-Huei Lin, Kun-Che Tsai, Ming-Feng Wei, Han-Min Tsai, Jau-Min Wong and Ming-Jium Shieh., *Bioconjugate Chem.* 2010, **21**, 679–689
- [44]. Wang, X., Chen, Q., & Lu, X., *Food Hydrocolloids*, 2014, **38**, 129-137.
- [45]. Bosio, VE., Machain, V., Lopez, AG., De Berti, IOP., Marchetti, SG., Mechetti, M., & Castro, GR., *Applied biochemistry and biotechnology*, 2012, **167**, 1365-1376.
- [46]. Chouhan, R., & Bajpai, AK., *Journal of nanobiotechnology*, 2009, **7**, 5.
- [47]. Park, Y., Hong, YN., Weyers, A., Kim, YS., & Linhardt, RJ., *Nanobiotechnology, IET*, 2011, **5**, 69-78.
- [48]. Iram, F., Iqbal, MS., Athar, MM., Saeed, MZ., Yasmeen, A., & Ahmad, R., *Carbohydrate polymers*, 2014, **104**, 29-33.
- [49]. Mohanty, RK., Thennarasu, S., & Mandal, AB., *Colloids and Surfaces B: Biointerfaces*, 2014, **114**, 138-143.
- [50]. Murawala, P., Phadnis, SM., Bhonde, RR., & Prasad, BLV., *Colloids and Surfaces B: Biointerfaces*, 2009, **73**, 224-228.
- [51]. Sun, IC., Na, JH., Jeong, SY., Kim, DE., Kwon, IC., Choi, K., Ahn, HC., & Kim, K., *Pharmaceutical research*, 2014, **31**, 1418-1425.
- [52]. Bar-Ilan, O., Albrecht, R. M., Fako, VE., & Furgeson, DY., *Small*, 2009, **5**, 897-910.
- [53]. Kumar, SSD., Surianarayanan, M., Vijayaraghavan, R., Mandal, AB., & MacFarlane, DR., *European Journal of Pharmaceutical Sciences*, 2014, **51**, 34-44.
- [54]. Browning, LM., Lee, KJ., Huang, T., Nallathamby, PD., Lowman, JE., & Xu, X. HN., *Nanoscale*, 2009, **1**, 138-152.
- [55]. Mirza, AZ., & Shamshad, H., *European journal of medicinal chemistry*, 2011, **46**, 1857-1860.
- [56]. Kievit, FM., Wang, FY., Fang, C., Mok, H., Wang, K., Silber, JR., Ellenbogen, RG., & Zhang, M., *Journal of Controlled Release*, 2011, **152**, 76-83.
- [57]. Madhusudhan, A., Reddy, GB., Venkatesham, M., Veerabhadram, G., Kumar, D. A., Natarajan, S., Yang, M.Y., Hu, H & Singh, SS., *International journal of molecular sciences*, 2014, **15**, 8216-8234.
- [58]. You, J., Zhang, G., & Li, C., *ACS nano*, 2010, **4**, 1033-1041.
- [59]. Shalviri, A., Raval, G., Prasad, P., Chan, C., Liu, Q., Heerklotz, H., Rauth, AM., & Wu, XY., *European Journal of Pharmaceutics and Biopharmaceutics*, 2012, **82**, 587-597.
- [60]. Ebrahimnejad, P., Dinarvand, R., Sajadi, A., Jaafari, MR., Nomani, A. R., Azizi, E., & Atyabi, F., *Nanomedicine: Nanotechnology, Biology and Medicine*, 2010, **6**, 478-485.
- [61]. Wang, Y., Li, P., Chen, L., Gao, W., Zeng, F., & Kong, LX., *Drug delivery*, 2015, **22**, 191-198.
- [62]. Nguyen, HN., Hoang, TMN., Mai, TTT., Nguyen, TQT., Do, HD., Pham, TH., & Ha, PT., *Advances in Natural Sciences: Nanoscience and Nanotechnology*, 2015, **6**, 025005.
- [63]. Sivagami, G., Vinothkumar, R., Preethy, CP., Riyasdeen, A., Akbarsha, MA., Menon, VP., & Nalini, N., *Food and Chemical Toxicology*, 2012, **50**, 660-671.
- [64]. Ho, K., Yazan, LS., Ismail, N., & Ismail, M., *Cancer epidemiology*, 2009, **33**, 155-160.
- [65]. D. Dutta, A. K. Sahoo, A. Chattopadhyay and S. S. Ghosh, J. Mater. Chem. B, 2015, DOI: 10.1039/C5TB01583A.
- [66]. Weinberg, R.A., *Cell*, 1995, **81**, 323–330.
- [67]. Sanchez-Martinez, C., Gelbert, L. M., Lallena, M. J., & de Dios, A., *Bioorganic & medicinal chemistry letters*, 2015, **11**, 291-302.
- [68]. Wang, Y.B., Qin, J., Zheng, X.Y., Bai, Y., Yang, K., & Xie, L.P., *Phytomedicine*, 2010, **17**, 363-8.
- [69]. Oliver, F. J., de la Rubia, G., Rolli, V., Ruiz-Ruiz, M. C., de Murcia, G., & Ménessier-de Murcia, J., *Journal of Biological Chemistry*, 1998, **273**, 33533-33539.



One pot aqueous green synthesis of gold nanoparticles (GNPs) decorated with folic acid and loaded with Doxorubicin suitable for anti-cancer drug delivery and were potentially promising as a new therapeutic system for cancer treatment.